

¹ PREPARED FOR SUBMISSION TO JINST

² ICFA BEAM DYNAMICS NEWSLETTER #83 — ADVANCED ACCELERATOR CONCEPTS / ICFA ANA

³ FERMILAB-PUB-22-137

⁴ SUBMITTED: MARCH 14, 2022

⁵ **On Possibility of Low-emittance High-energy Muon 6 Source Based on Plasma Wakefield Acceleration**

⁷ **Vladimir Shiltsev** ^{a,1}

⁸ *^aFermi National Accelerator Laboratory, Batavia, Illinois 60510, USA*

⁹ *E-mail: shiltsev@fnal.gov*

¹⁰ **ABSTRACT:** Plasma wakefield acceleration (PWA) channels are characterized by very high accelerating gradients and very strong focusing fields. We propose to employ these properties for effective ¹¹ production of low emittance high energy muon beams, consider muon beam dynamics in the PWFA ¹² cell and analyze various options and potential of the PWA-based muon sources. ¹³

¹⁴ **KEYWORDS:** Wake-field acceleration (laser-driven, electron-driven), Targets (spallation source tar-¹⁵ gets, radioisotope production, neutrino and muon sources), Beam dynamics, Accelerator subsystems ¹⁶ and technologies

¹This manuscript has been authored by Fermi Research Alliance, LLC under Contract No. DE-AC02-07CH11359 with the U.S. Department of Energy, Office of Science, Office of High Energy Physics.

17 **Contents**

18	1	Introduction	1
19		1.1 Challenges of muon production	1
20	2	PWA-based muon source	3
21		2.1 Acceleration by plasma wake-fields	3
22		2.2 Muons in PWA channel	4
23		2.3 Possible production schemes	5
24	3	Discussion	8

25 **1** **Introduction**

26 The muon was discovered almost hundred years ago, but still remains of a profound and growing
27 interest for particle physics (see, e.g. [1]). About 200 times heavier than electron, the muon is now
28 part of the second generation of particles of the Standard Model of elementary particles, together
29 with muon neutrino and the strange s and the charm c quarks. The Standard Model is proven to
30 describe processes at the distances $O(10^{-19} \text{ m})$ but is predicted to break at the Planck scale $O(10^{-35}$
31 $\text{m})$. Muons are used to search for processes beyond the Standard Model, such as possible rare muon
32 decays and muon to electron conversion, possible muonium-antimuonium conversion, decays of the
33 B -meson into a muon pair. Muons are in the heart of other puzzles, like the *proton radius puzzle*,
34 anomalous magnetic and dipole muon moments and rare processes initiated by muon.

35 Applications of muon beams range from chemistry (where the muonium atom is a true light
36 version of hydrogen) to condensed matter physics, where the muon spin spectroscopy, also known
37 as μ SR, helps to study properties semiconductors, magnetism, superconductivity and quantum
38 diffusion; to exploration of alternative energy source within the framework of muon catalyzed
39 fusion (μ CF) and discoveries at the particle physics energy frontier envisioned with future muon
40 colliders.

41 All these research and applications greatly depend on effective generation of muon beams,
42 some requiring high intensity, others high energy or low emittances, while, for example, neutrino
43 factories and muon colliders requiring it all - high intensity, low emittance, high-energy muon
44 beams [2, 3].

45 **1.1 Challenges of muon production**

46 The main challenge to produce muons is that they are not stable particles having lifetime of $2.2 \mu\text{s}$
47 in the muon rest frame before decaying into an electron, a muon-type neutrino, and an electron-type
48 antineutrino ($\mu^- \rightarrow e^- \nu_\mu \bar{\nu}_e$). Therefore, other stable particles, such as electrons, photons or protons
49 are required to generate muons as either secondary or even tertiary reaction product. The most

common is production chain $p \rightarrow \text{target} \rightarrow \pi^+(\pi^-) \rightarrow \mu^+(\mu^-)$ in which the pions (and subsequent muons) are produced with large transverse angular spread $\theta \simeq m_\pi/P_\pi O(1)$ and efficient collection requires strong downstream focusing elements that can keep the secondaries confined within limited aperture. Spreads of longitudinal momenta of the pions and muons are quite large, too.

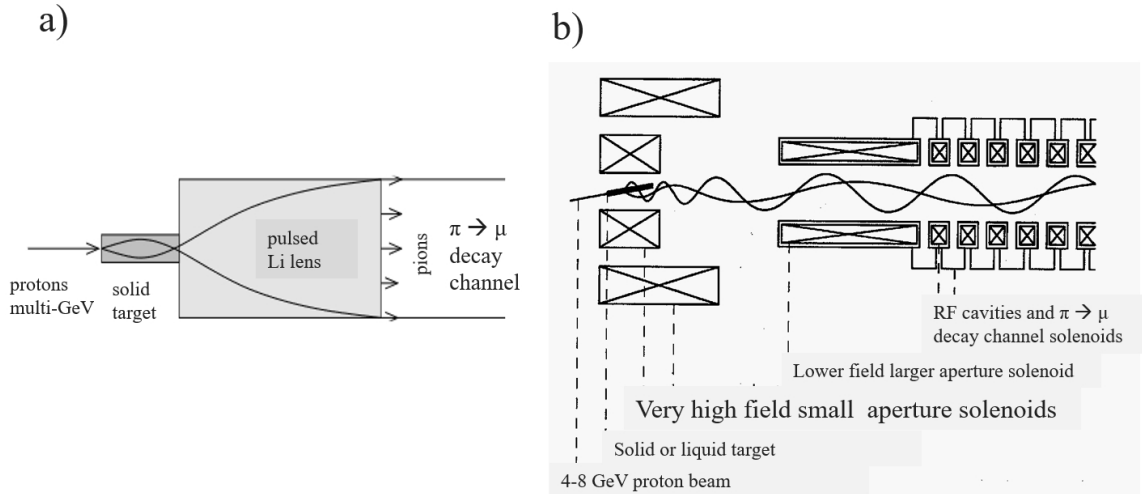


Figure 1. Muon production schemes: a) using pulsed short-focus Lithium lens for collection of pions, which later decay into muons; b) using very high field SC solenoids for pion capture, followed by RF acceleration section.

Fig. 1 illustrates schematically two options. In the first one, pulsed short-focus Lithium lens is used for collection of pions, which later decay into muons. The method is employed, e.g., to get high energy beam of polarized muons for the muon $g - 2$ experiment [4] and has an efficiency of conversion of 8 GeV protons into 3.1 GeV muons of about $2 \cdot 10^{-7}$ for the downstream accelerator beamline acceptance $O(1\%)$ [5]. The production system of the Fermilab Muon Campus includes Inconel target, followed by Lithium Lens with pulsed 116 kA current, producing a magnetic field gradient of 232 T/m located 0.3 m downstream the target. The Lithium Lens has the advantage over conventional quadrupoles in that it focuses in both transverse planes and produces an extremely strong magnetic field.

The most challenging are requirements of a future muon collider. Its muon source uses very high field SC solenoids for pion capture, followed by RF acceleration section. A high power proton beam out of 4-8 GeV 2-4 MW SRF H^- linac goes through pre-target accumulation and compressor rings where high-intensity 1-3 ns long proton bunches are formed. At $O(5 \text{ Hz})$ rate, one of several of such bunches hit liquid mercury target for converting the proton beam into a tertiary muon beam with energy of about 200 MeV. The $p \rightarrow \mu$ conversion efficiency is very high $O(10\%)$ but resulting transverse normalized emittance of the muon beams are huge $O(0.1 \text{ m rad})$ and a sophisticated multi-stage ionization cooling section is required to reduce the transverse and longitudinal emittances by a factor of 10^6 (for 6D emittance) and to make the beams suitable for a multistage acceleration and, eventually, high luminosity $\mu^+\mu^-$ collisions.

A complete cooling channel for high luminosity muon collider would be $O(1 \text{ km})$ long and consist of $O(30)$ cooling stages, each yielding about a factor of 2 in 6D phase space reduction.

75 The ionization cooling method, though relatively straightforward in principle, faces some practical
 76 implementation challenges. These include RF breakdown suppression and attainment of high
 77 accelerating gradients in relatively low frequency NC RF cavities immersed in strong magnetic
 78 fields. The International Muon Ionization Cooling Experiment (MICE) [6] at RAL (UK) has
 79 recently demonstrated effective $O(10\%)$ reduction of transverse emittance of initially dispersed 140
 80 MeV/c muons passing through an ionization cooling channel cell consisting of a sequence of LiH or
 81 liquid hydrogen absorbers within a lattice of up to 3.5 T solenoids that provide the required particle
 82 focusing.

83 2 PWA-based muon source

84 Plasma wakefield acceleration (PWA) channels are characterized by very high accelerating gradients
 85 and very strong focusing fields. These properties can be used for effective production of low
 86 emittance high energy muon beams.

87 2.1 Acceleration by plasma wake-fields

88 Ionized plasmas can sustain electron plasma density waves with electric fields in excess of $E_0 =$
 89 $cm_e\omega_p/e$ or

$$E_0 \approx 96 \text{ [V/m]} \sqrt{n_0 \text{ [cm}^{-3}]}, \quad (2.1)$$

90 (so-called *cold nonrelativistic wave-breaking field* [7]) where n_0 denotes the ambient electron
 91 number density, $\omega_p = k_p c = \sqrt{e^2 n_0 / (m_e \epsilon_0)}$ the electron plasma frequency, m_e and e electron rest
 92 mass and charge, respectively, c the speed of light in vacuum, and ϵ_0 the electrical permittivity of
 93 free space. For example, a plasma density of about 10^{18} cm^{-3} yields $E_0 \sim 100 \text{ GV/m}$, approximately
 94 three orders of magnitude greater than $\sim 100 \text{ MV/m}$ obtained in conventional breakdown limited
 95 RF structures. Such gradients can be effectively excited by either powerful external pulses of
 96 laser light or by electron bunches if they are shorter than the plasma wavelength $\lambda_p = c/\omega_p \approx$
 97 $33 \mu\text{m} \times \sqrt{10^{18} \text{ cm}^{-3} / n_0}$, or by longer beams of charged particles if their charge density is modulated
 98 with the period of λ_p .

99 There are several regimes of laser-driven plasma acceleration that may be accessed based on
 100 the intensity of the short laser pulses or electron bunches. *Quasi-linear regime* takes place in the
 101 case of low intensity drivers, while for the high intensities the plasma channel sustains, so called
 102 *bubble regime*, where (almost) all the electrons are expelled by either the drive e^- beam or by the
 103 laser ponderomotive force, forming an ion cavity co-propagating behind the laser. The structure of
 104 wakefield forces inside the ion cavity in the bubble regime is (see, eg [8])

$$F_z = eE_0 k_p \zeta / 2, \quad F_r = e(E_r - B_\theta) = -eE_0 k_p r / 2 \quad (2.2)$$

105 Here $\zeta = z - ct$ is co-moving longitudinal coordinate ($\zeta=0$ marks the center of the ion cavity)
 106 and r the radial coordinate. One can see that the accelerating force F_z is independent of the
 107 transverse position and the focusing force F_r linear with r . The transverse size of the bubble is
 108 about $r_{max} \approx 3/k_p \approx \lambda_p/2$. The focusing forces of the plasma bubble in 10^{18} cm^{-3} plasma are
 109 equivalent to those for $G = E_0 k_p / 2 \approx 0.3 \text{ MT/cm} (n_p / 10^{18}) \sim 300 \text{ kT/cm}$ gradients.

110 Naturally, the transverse fields in the ion cavity are defocusing for positively charge particle;
 111 hence, stable acceleration of, e.g., e^+ of μ^+ particles can not occur in the bubble regime and either
 112 the quasi-linear regime of operation or wakefield excitation in hollow plasma channels is needed.

113 So far, the primary advantage that a plasma wakefield accelerator could present was considered
 114 to be its compactness and, correspondingly, short length of, e.g., high energy e^+e^- collider. Collisions of intrinsically short bunches (a fraction of the plasma wavelength) are also advantageous for
 115 the reduction of beamstrahlung effects in plasma-based $O(1 \text{ TeV})$ cme e^+e^- colliders.

116 Strong focusing forces of the PWA channels have been proposed for use in the final focus systems
 117 of the future linear e^+e^- colliders (*plasma lenses* [9–11]), but they also can help in production and
 118 efficient collection of secondary particles, such as muons.

120 2.2 Muons in PWA channel

121 Let us consider a muon born in plasma wake-field channel - see Fig.2. Equation of motion in the
 122 longitudinal degree of motion:

$$123 \frac{dp_z}{dt} = F_z, \quad (2.3)$$

124 where the muon momentum $p_z = \gamma_\mu \beta_\mu m_\mu$, naturally yields approximately linear growth of the
 muon's energy

$$\gamma_\mu = 1 + z\kappa e E_0 / m_\mu c^2 \approx z\kappa k_p (m_e / m_\mu). \quad (2.4)$$

125 For simplicity one can assume that particles quickly get relativistic ($\beta \approx 1$ and $dt = dz/c$, and
 126 optimal position ζ for the fastest acceleration corresponding to $\kappa \approx 2$.

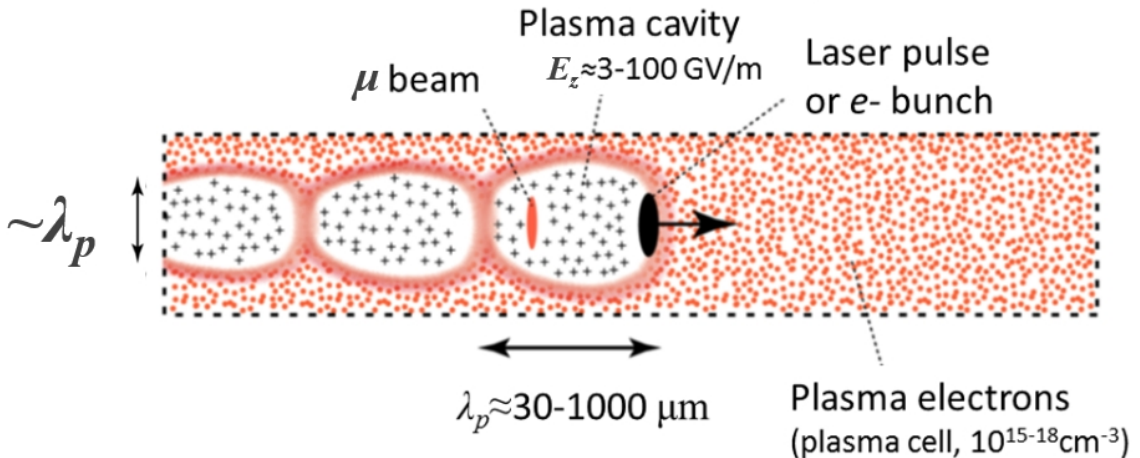


Figure 2. Conceptual scheme of the plasma-wakefield acceleration muon source.

127 In the transverse plane, the equation reads:

$$\frac{dp_r}{dt} = m_\mu c^2 \frac{d}{dz} \left(\gamma_\mu(z) \frac{dr}{dz} \right) = -e E_0 \frac{k_p r}{2}. \quad (2.5)$$

128 The exact solution is:

$$r(z) = c_1 J_0 \left(2 \sqrt{\frac{z\pi}{\kappa\lambda_p}} \right) + c_2 Y_0 \left(2 \sqrt{\frac{z\pi}{\kappa\lambda_p}} \right). \quad (2.6)$$

129 It describes betatron oscillations with diminishing amplitude $r(z) \propto \exp(izk_\mu(z))$. Of importance
 130 for us is that the betatron oscillations are fast compared to the rate of acceleration. Indeed, the
 131 betatron-function $\beta_\mu = 1/k_\mu \approx \lambda_p \sqrt{2\gamma_\mu m_\mu/m_e}$ (assuming negligible beam loading) and the
 132 fractional energy increase over the betatron oscillation period $\Delta\gamma_\mu/\gamma_\mu$ is small:

$$\frac{\Delta\gamma_\mu}{\gamma_\mu} = \frac{2\pi\beta_\mu\kappa k_p(m_e/m_\mu)}{\gamma_\mu} = 2\pi\kappa\sqrt{\frac{2m_e}{\gamma_\mu m_\mu}} \lesssim \frac{0.1}{\sqrt{\gamma_\mu}}. \quad (2.7)$$

133 Therefore, the transverse motion is adiabatic, the period of the muon oscillations grows as $\sqrt{\gamma_\mu} \propto \sqrt{z}$
 134 while the amplitude slowly diminishes as $|r| \approx r_{max}\sqrt{\beta_\mu/\gamma_\mu} \propto r_{max}/\gamma_\mu^{1/4}$. The maximum angular
 135 deviation $\theta = dr/dz$ and the maximum amplitude relate to each other as $\theta_{max} = r_{max}/\beta_\mu$ and if
 136 the latter is limited by the transverse size of the bubble $r_{max} \simeq \lambda_p/2$, then

$$\theta_{max} = r_{max}/\beta_\mu = \pi\sqrt{\frac{m_e}{2\gamma_\mu m_\mu}} \approx \frac{0.15}{\sqrt{\gamma_\mu}}, \quad (2.8)$$

137 that defines the maximum normalized acceptance ϵ_μ^{max} of the muons captured and accelerated in
 138 the PWA channel:

$$\epsilon_\mu^{max} = \gamma_\mu \theta_{max} r_{max} = \lambda_p \gamma_\mu^{1/4} \sqrt{\frac{m_e \pi^2}{8m_\mu}} \approx 0.078 \lambda_p. \quad (2.9)$$

139 This equation indicates that the limit is set by the dynamics at low energies $\gamma_\mu \sim 1$ and gives the
 140 estimated normalized emittance of the accelerated muon beam $\epsilon_\mu^{max} \approx 2.6 \mu\text{m}$ for dense gaseous
 141 plasma $n_e = 10^{18} \text{ cm}^{-3}$ and about 8-20 nm for solid state plasma $n_e = 10^{22-23} \text{ cm}^{-3}$. In the first
 142 case, acceleration of muons to, say, 10 GeV, would require $O(10 \text{ cm})$ PWA channel, while in the
 143 case of a crystal it can be done over $O(1 \text{ mm})$. To be noted, some emittance growth may occur
 144 by elastic scattering of the beam muon against the background ions in the plasma, but as shown
 145 elsewhere – see, e.g., Ref.[8] – the strong focusing in the plasma bubble suppresses the growth. The
 146 effect is almost independent on the plasma density and is very small even for electrons, while for
 147 muons it is negligible due to additional suppression factor (m_e/m_μ) .

148 Of course, these estimates look extremely attractive if compared to the most sophisticated
 149 muon production, ionization cooling and initial acceleration complex of a muon collider that
 150 requires kilometers of magnets and RF cavities to get $O(10 \text{ GeV})$ muons with one to three orders
 151 of magnitude higher normalized transverse emittances $O(30 \mu\text{m})$.

152 2.3 Possible production schemes

153 Practical applications of the proposed PWA-based low-emittance high-energy muon sources criti-
 154 cally depend on the muon intensity. Obviously, to take advantage of the fast acceleration and strong
 155 focusing, the muons should be produced inside the plasma bubble or in its vicinity $O(\lambda_p)$. One can
 156 think of three process that can make that:

- 157 a) photoproduction: high energy γ 's or electrons on target $\rightarrow \mu^+(\mu^-)$;
- 158 b) "standard" production scheme described above in the introduction: protons \rightarrow target \rightarrow pions
 $\rightarrow \mu^+(\mu^-)$;
- 160 c) generation of "prompt" muons: protons \rightarrow target \rightarrow vector mesons $\rightarrow \mu^+(\mu^-)$.

161 In all these schemes the external primary beam can be injected into the plasma channel together

162 (simultaneously and in the same location) with external plasma drivers (electron bunch or laser
 163 pulse) - see Fig.3. Note, that plasma wakefield oscillations are essentially low- Q , so only one of
 164 few plasma periods/bubble can be employed to generate few short muon bunches. Also, the bubble
 165 wake field might be distorted (loaded) by high intensity primary beams and secondary particles
 166 (e^+/e^- , pions, kaons, etc).

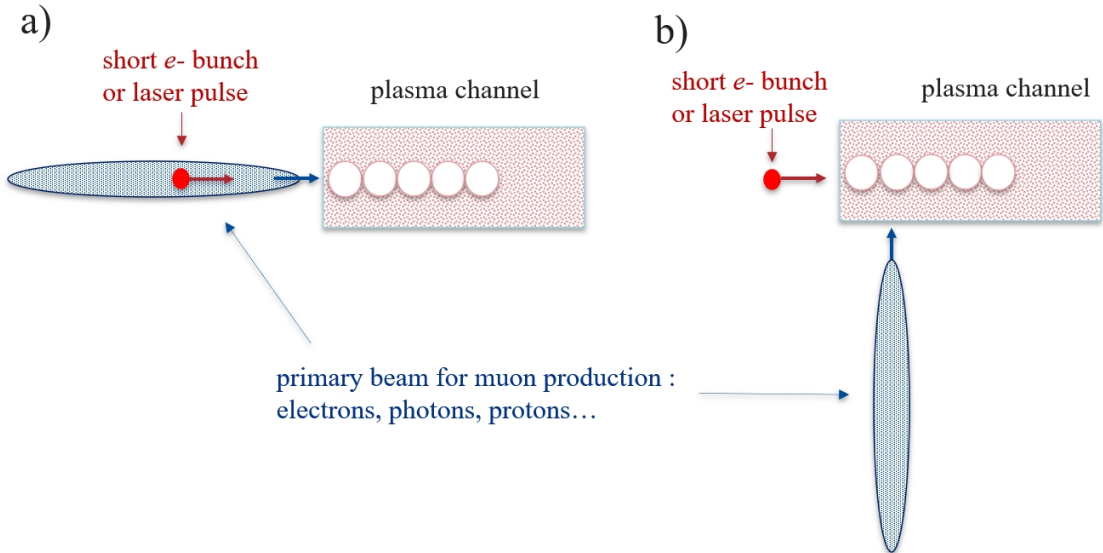


Figure 3. Muon PWA source : possible schemes for simultaneous injection of plasma wakefield drivers (laser pulses or short electron bunches) and primary beams needed for muon generation: a) collinear; b) orthogonal.

167 All these schemes have serious challenges, some of them considered in [12]. The photoproduction
 168 via Bethe-Haitler (BH) reaction $\gamma + Z \rightarrow \mu^+ \mu^- + Z$ has small cross-section. Photons
 169 need to have energy far exceeding the muon production threshold of 210 MeV and can be obtained
 170 via bremsstrahlung of multi-GeV electron beam in the target. Similar BH-channel efficiency for
 171 the positron production is $O(1\%) e^+/e^-$. For the muon pair production, the BH cross-section is
 172 $(m_e/m_\mu)^2 = 1/40000$ times smaller - so, not only that muon efficiency will be $O(10^{-5-6})$ but also
 173 one should expect significant loading of the plasma bubble by much more numerous electrons and
 174 positrons.

175 Even smaller are cross-sections of the muon pair production via e^+e^- annihilation $\sigma =$
 176 $87\text{nb/s(GeV}^2)$ and even with most optimistic luminosity assumptions the production rate will
 177 be in sub-Hz regime [13].

178 Muon production cross-sections via photo-meson reaction and proton-nucleon reactions can be
 179 quite high $O(100 \text{ mb})$ and conversion efficiencies can indeed be high, but the problem is two fold:
 180 a) proton bunches are usually much longer $O(1 - 10\text{cm})$ and only a small fraction of proton beam
 181 can interact with plasma when the short sequence of bubbles exist in the plasma after the passage
 182 of drive laser pulse or short electron bunch; b) also, the immediate products of these reactions are
 183 mesons (pions and kaons) and takes long time and distance for them to decay into muons. For
 184 charge pions it is $\tau = 26 \text{ ns}$ ($c\tau = 7.8 \text{ m}$) and, correspondingly, these pions should stay in the plasma

185 channel for that long to decay that creates additional difficulties.

186 There are fast decay options, eg $\pi^0 \rightarrow \gamma\gamma$ ($\tau = 85$ as with follow up photons possibly
 187 generation muons is of high enough energy. That would require very high energy primary proton
 188 beams $O(100 \text{ GeV})$. Similarly, fast decays via vector bosons (e.g., D 's) and generation of so called
 189 *prompt muons* offer another opportunity [14–16]. These reactions might have relatively high (still
 190 small) cross-section $O(1 \text{ mub})$ and might require very high energy of primary protons $O(100\text{-}1000$
 191 GeV). Practicality of these and other possible muon generation schemes for the PWA-based muon
 192 sources requires further, more detail examination.

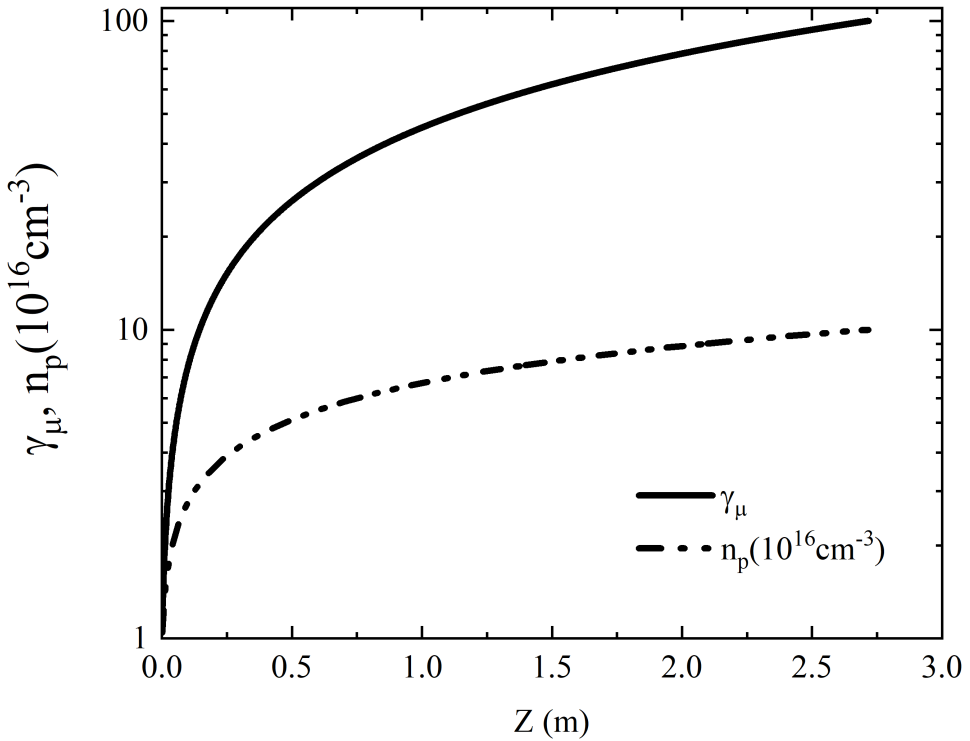


Figure 4. Plasma density and muon energy in tapered PWA-based 10 GeV muon source with normalized acceptance of 25 μm .

193 The PWA-based scheme can be modified to maximize the acceptance of the accelerated beam.
 194 For that, a gradual increase of the plasma density $n_e(z)$ is needed. E.g., if one takes the desired
 195 normalized acceptance of ϵ_μ^{max} then according to Eq.2.9, in order to keep it constant along the
 196 channel, the plasma wavelength should scale as:

$$\lambda_p(z) = \lambda_p^0 \gamma_\mu(z)^{-1/4}, \quad (2.10)$$

197 where initial plasma density should correspond to initial wavelength of $\lambda_p^0 = \epsilon_\mu^{max}/0.078$. Solution

198 of (2.10) is trivial, taking into account Eq.(2.4):

$$n_p(z) = n_p^0 (1 + \alpha z)^{2/5}, \gamma_\mu(z) = (1 + \alpha z)^{4/5}, \quad (2.11)$$

199 where $\alpha = (5\pi\kappa m_e)/(2\lambda_p^0 m_\mu)$. Fig.4 presents calculated density profile for a 2.5 m long 10 GeV
200 muon source with $\epsilon_\mu^{max} = 25\mu\text{m}$ (corresponding to $\lambda_p^0 = 0.33$ mm and $n_p^0 = 10^{16} \text{ cm}^{-3}$).

201 3 Discussion

202 The proposed muon source based on plasma wakefield acceleration looks very attractive because of
203 the promise of very small emittance high energy muon beams in an ultimately small footprint. Our
204 analysis above indicates normalized emittances possible in the range of $\mu\text{m rad}$ to nm rad , depending
205 on the plasma density (ϵ_n is proportional to the plasma wavelength λ_p). That surely would be very
206 welcome development not only for advanced schemes (such as linear crystal channeling muon
207 collider [17]) but also in traditional muon colliders as it would eliminate the most complex muon
208 production, ionization cooling and early acceleration parts of multi-TeV muon collider. Of course,
209 acceleration and focusing of positively charged muons μ^+ will be as challenging as for positrons in
210 the advanced laser-plasma and beam-driven plasma wakefield accelerators.

211 Even the first look into the proposed muon sources indicates significant challenge as most
212 potential applications require both small emittances and high intensity (i.e., high-brightness) muon
213 beams, and that needs to be studied in detail and the most promising options identified and analyzed.

214 For completeness, one has to mention that due to growing interest in high brightness muon
215 beams, several other novel schemes have been recently proposed, such as a) the *positron-driven*
216 *muon production* scheme that envisions 45 GeV positrons hitting a target to generate muon pairs
217 through e^+e^- annihilation just above threshold [18], allowing low emittance beams to be obtained
218 directly, without any cooling [19]; and b) the *Gamma Factory* (GF) [20] that could potentially
219 generate frequent bursts of gamma rays by repeatedly colliding a partially stripped heavy-ion beam
220 circulating in the LHC, or in a future higher-energy hadron storage ring like the FCC-hh, with a
221 conventional laser pulse, profiting from two Lorentz boosts. Being sent on a suitable target, the
222 GF's intense bursts $O(1 \text{ GeV})$ gamma could produce muons at an high rate. Thereby, the GF could
223 deliver positrons at the rate required for the aforementioned positron-based muon production, or,
224 alternatively, it could directly provide a low-emittance muon beam [21].

225 Practicality of these schemes is under active exploration, which might be synergistically helpful
226 to follow-up studies of the PWA-based high brightness high energy muon sources proposed in his
227 paper.

228 Acknowledgments

229 Author greatly appreciates helpful discussions with M. Palmer, K. Yonehara and N. Mokhov on
230 various aspects of the proposed scheme. This manuscript has been authored by Fermi Research
231 Alliance, LLC under Contract No. DE-AC02-07CH11359 with the U.S. Department of Energy,
232 Office of Science, Office of High Energy Physics.

233 **References**

234 [1] *Modern Muon Physics: Selected Issues*.

235 [2] S. Geer, *Muon colliders and neutrino factories, Annual Review of Nuclear and Particle Science* **59**
236 (2009) 347.

237 [3] K.R. Long, D. Lucchesi, M.A. Palmer, N. Pastrone, D. Schulte and V. Shiltsev, *Muon colliders to*
238 *expand frontiers of particle physics, Nature Physics* **17** (2021) 289.

239 [4] B. Abi, T. Albahri, S. Al-Kilani, D. Allspach, L. Alonzi, A. Anastasi et al., *Measurement of the*
240 *positive muon anomalous magnetic moment to 0.46 ppm, Physical Review Letters* **126** (2021) 141801.

241 [5] D. Stratakis, M. Convery, J. Morgan, D. Still, M. Syphers and V. Tishchenko, *Simulated performance*
242 *of the production target for the muon g-2 experiment, arXiv preprint arXiv:1709.07838* (2017) .

243 [6] M. Bogomilov et al., *Demonstration of cooling by the muon ionization cooling experiment, Nature*
244 **578** (2020) 53.

245 [7] J.M. Dawson, *Nonlinear electron oscillations in a cold plasma, Physical Review* **113** (1959) 383.

246 [8] C. Schroeder et al., *Beam dynamics challenges in linear colliders based on laser-plasma accelerators,*
247 **JINST this Special Issue** .

248 [9] P. Chen, *Grand disruption: A possible final focusing mechanism for linear colliders, Part. Accel.* **20**
249 (1986) 171.

250 [10] J. Su, T. Katsouleas, J. Dawson and R. Fedele, *Plasma lenses for focusing particle beams, Physical*
251 *Review A* **41** (1990) 3321.

252 [11] E. Chiadroni, M. Anania, M. Bellaveglia, A. Biagioni, F. Bisesto, E. Brentegani et al., *Overview of*
253 *plasma lens experiments and recent results at SPARC_LAB, Nuclear Instruments and Methods in*
254 *Physics Research Section A: Accelerators, Spectrometers, Detectors and Associated Equipment* **909**
255 (2018) 16.

256 [12] A.A. Sahai, T. Tajima and V.D. Shiltsev, *Schemes of laser muon acceleration: Ultra-short,*
257 *micron-scale beams, International Journal of Modern Physics A* **34** (2019) 1943008.

258 [13] *dimus*, Tech. Rep.

259 [14] H. Kasha, R. Kellogg, M. Lauterbach, R. Adair, L. Leipuner, R. Larsen et al., *Evidence of pair origin*
260 *of prompt muons, Physical Review Letters* **36** (1976) 1007.

261 [15] W. Morse, K.-W. Lai, R. Larsen, Y. Lee, L. Leipuner, D. Lowenstein et al., *Properties of prompt*
262 *muons produced by 28 gev proton interactios, in AIP Conference Proceedings, vol. 45, pp. 129–137,*
263 *American Institute of Physics, 1978.*

264 [16] R. Stroynowski, *Lepton pair production in hadron collisions, Physics Reports* **71** (1981) 1.

265 [17] V.D. Shiltsev, *High-energy particle colliders: past 20 years, next 20 years, and beyond,*
266 *Physics-Uspekhi* **55** (2012) 965.

267 [18] M. Antonelli, M. Boscolo, R. Di Nardo and P. Raimondi, *Novel proposal for a low emittance muon*
268 *beam using positron beam on target, Nuclear Instruments and Methods in Physics Research Section*
269 *A: Accelerators, Spectrometers, Detectors and Associated Equipment* **807** (2016) 101.

270 [19] M. Boscolo, J.-P. Delahaye and M. Palmer, *The future prospects of muon colliders and neutrino*
271 *factories, in Reviews of Accelerator Science and Technology: Volume 10: The Future of Accelerators,*
272 *pp. 189–214, World Scientific (2019).*

273 [20] M.W. Krasny, *The gamma factory proposal for CERN*, arXiv preprint arXiv:1511.07794 (2015) .

274 [21] F. Zimmermann, *Future colliders for particle physics—“big and small”*, *Nuclear Instruments and*
275 *Methods in Physics Research Section A: Accelerators, Spectrometers, Detectors and Associated*
276 *Equipment* **909** (2018) 33.